# Aerosol chemical speciation from EPIC

Sujung Go[1,2], Myungje Choi[1,2], Gregory L. Schuster[3], and Alexei Lyapustin[2]

1) UMBC JCET, 2) NASA GSFC, 3) NASA Langley

# Publications - the presentation contains the work of 3 papers

1) Lyapustin. A., Go. S., Korkin. S., Wang. Y., Torres. O., Jethva. H. and Marshak. A. (2021) Retrievals of Aerosol Optical Depth and Spectral Absorption from DSCOVR EPIC. *Front. Remote Sens.* 2:645794. doi: 10.3389/frsen.2021.645794.

2) Go, S., Lyapustin, A., Schuster, G. L., Choi, M., Ginoux, P., Chin, M., Kalashnikova, O., Dubovik, O., Kim, J., Silva, A. D., Holben, B., and Reid, J. S.: Inferring iron oxides species content in atmospheric mineral dust from DSCOVR EPIC observations, *Atmos. Chem. Phys. Discuss.* [preprint], https://doi.org/10.5194/acp-2021-599, in review, 2021.

3) Choi, M., A. Lyapustin, G. Schuster, S. Go, et al. Retrieval of BC and BrC smoke aerosol components from DSCOVR EPIC, *Atmos. Chem. Phys.* (to be submitted, 2021).

# Brief introduction

- The variability of spectral aerosol absorption (*k(λ)*) in UV-visible is caused by differences in aerosol chemical composition; the mineral dust absorption is mainly caused by hematite and goethite, whereas BrC and BC are responsible for the smoke absorption.

- **(Dust)** The iron-oxide (hematite and goethite) content of dust in the atmosphere and most notably its apportionment between hematite (α-$Fe_2O_3$) and goethite (α-FeOOH) are key determinants in quantifying dust's light absorption, its top of atmosphere UV radiances used for dust monitoring, and ultimately shortwave dust direct radiative effects (DRE). Li et al. (2021) quantified the range in dust DRE at the top of the atmosphere (TOA) due to current uncertainties in the surface soil mineralogical content using a dust mineral resolving climate model. It highlights the importance of distinguishing goethite from hematite for the shortwave dust DRE estimate. Otherwise, the model tends to underestimate dust warming at the TOA by ∼56%.

- **(Smoke)** Global warming gives rise to extending dry conditions in soil and vegetation, resulting in more frequent and severe wildfires that have been forecasted and observed over the last decades (Liu et al., 2010; Dennison et al., 2014). Chemical components information such as black carbon (BC) and brown carbon (BrC) will help improve representation of smoke in climate models, mapping of absorption to different fuel types, understanding of absorption changes with distance from the source, improve modeling of local tropospheric photochemistry (e.g., surface ozone) and surface UV irradiance.

# Brief Introduction

## Block-diagram of MAIAC EPIC algorithm

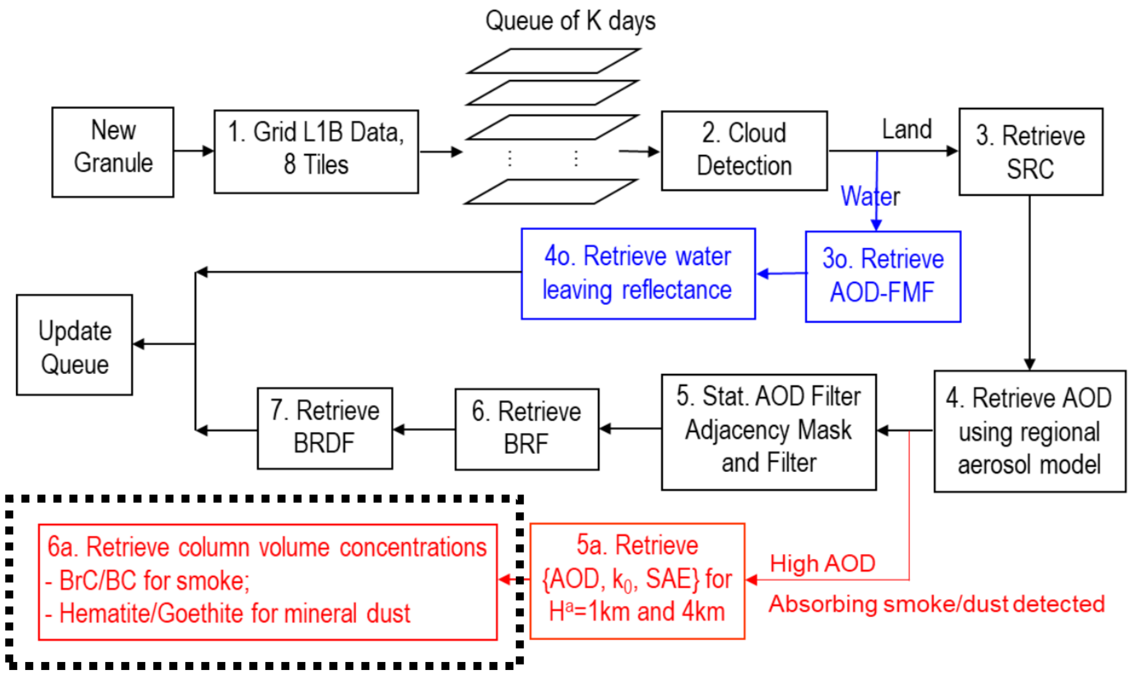

Queue of K days

New Granule

1. Grid L1B Data, 8 Tiles

2. Cloud Detection

Land

Water

3. Retrieve SRC

3o. Retrieve AOD-FMF

4o. Retrieve water leaving reflectance

Update Queue

4. Retrieve AOD using regional aerosol model

5. Stat. AOD Filter Adjacency Mask and Filter

6. Retrieve BRF

7. Retrieve BRDF

High AOD

Absorbing smoke/dust detected

5a. Retrieve {AOD, $k_0$, SAE} for $H^a$=1km and 4km

6a. Retrieve column volume concentrations
- BrC/BC for smoke;
- Hematite/Goethite for mineral dust

- Absorption of hematite and BrC strongly increase from Red towards UV. At the same time, absorption of BC is spectrally neutral and absorption by goethite weakly decreases towards UV.
- Speciate dust aerosol → hematite, goethite
- Speciate smoke aerosol → BC, BrC

## Refractive index of soil mineralogy component

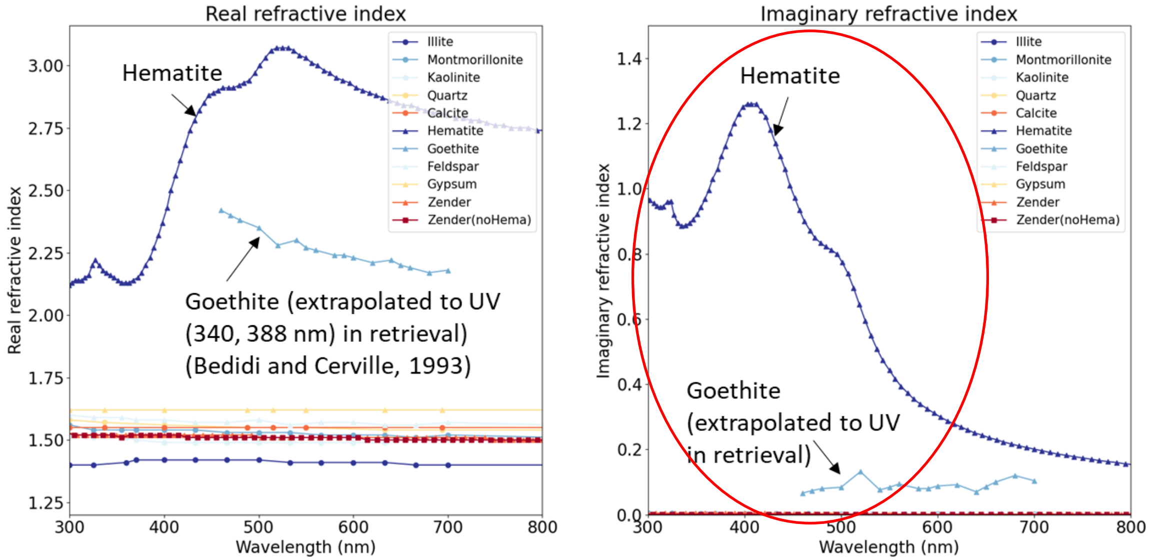

Hematite

Goethite (extrapolated to UV (340, 388 nm) in retrieval) (Bedidi and Cerville, 1993)

Hematite

Goethite (extrapolated to UV in retrieval)

## Refractive index of BC/BrC/SNA (Sulfate-Nitrate-Ammonium)

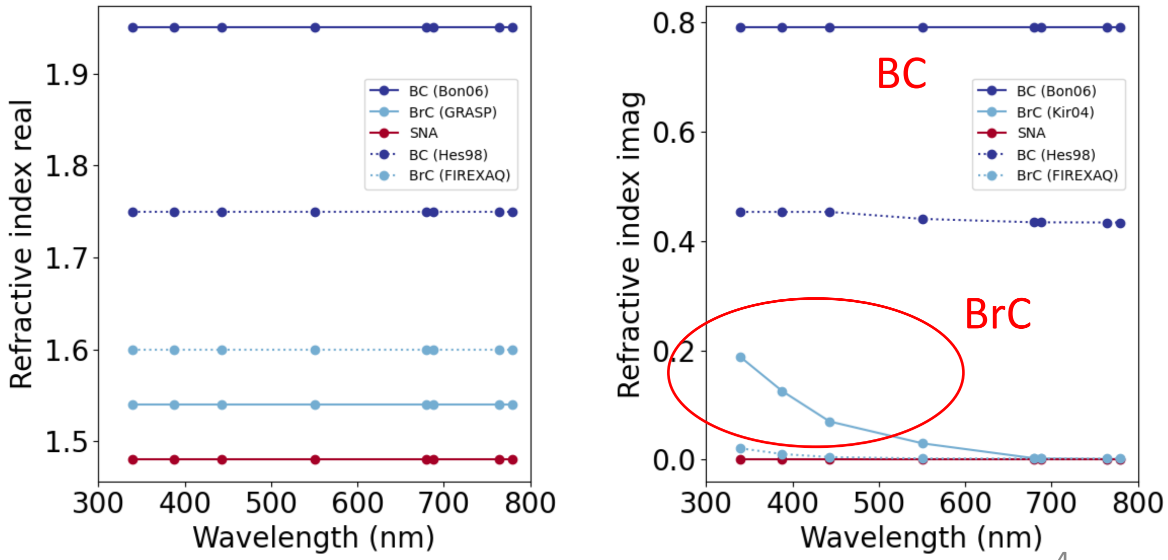

BC

BrC

# Methodology

Illustration of Maxwell Garnett effective medium approximation (**pure dust/smoke**)
(Bohren and Huffman, 1987; Schuster et al., 2016)

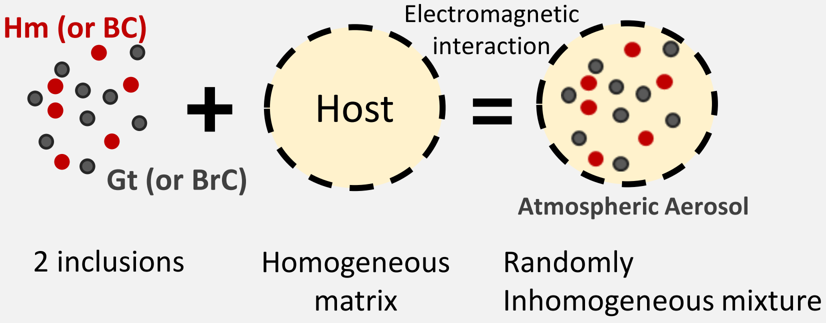

- $f_1$, $f_2$ : volume fraction of inclusions
- $\varepsilon_1$, $\varepsilon_2$, $\varepsilon_h$: complex dielectric function

$$\varepsilon_{MG} = \varepsilon_h \left[ 1 + \frac{3\left( f_1 \frac{\varepsilon_1 - \varepsilon_h}{\varepsilon_1 + 2\varepsilon_h} + f_2 \frac{\varepsilon_2 - \varepsilon_h}{\varepsilon_2 + 2\varepsilon_h} \right)}{1 - f_1 \frac{\varepsilon_1 - \varepsilon_h}{\varepsilon_1 + 2\varepsilon_h} - f_2 \frac{\varepsilon_2 - \varepsilon_h}{\varepsilon_2 + 2\varepsilon_h}} \right] = (n_{mix} + ik_{mix})^2$$

$$k_{mix} = \sqrt{\frac{\sqrt{{\varepsilon_{MG,r}}^2 + {\varepsilon_{MG,i}}^2} - \varepsilon_{MG,r}}{2}}$$

$$\chi^2 = \sum_{j=1}^{4} \left[ \frac{\left( k_{epic}(\lambda_j) - k_{mix}(\lambda_j) \right)^2}{k_{epic}(\lambda_j)} \right] \rightarrow min$$

- **Fitting $k_{epic}$ part only,** because MAIAC EPIC does not retrieve real refractive index ($n_{epic}$)

## Volume fraction range of (a) Goethite, (b) Hematite, as a function of $k_{680}$ and SAE(=$b$)

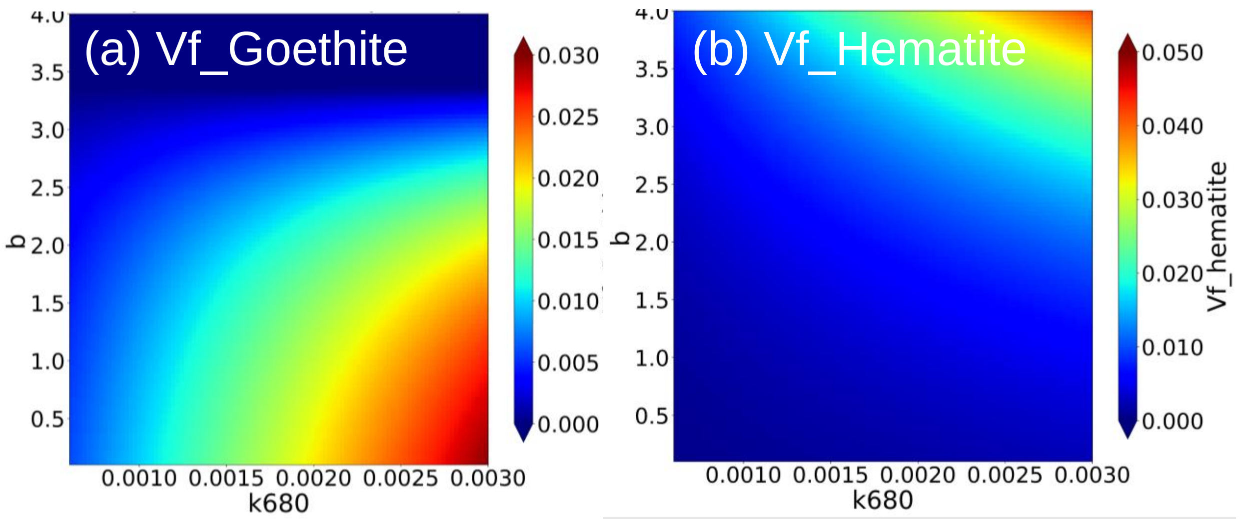

## Volume fraction range of (a) BC, (b) BrC, as a function of $k_{680}$ and SAE

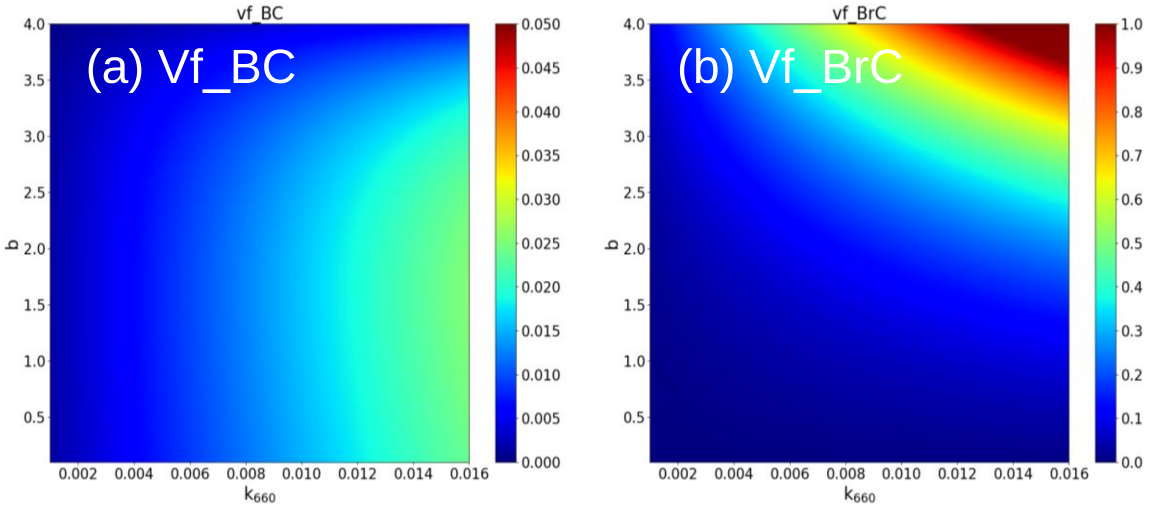

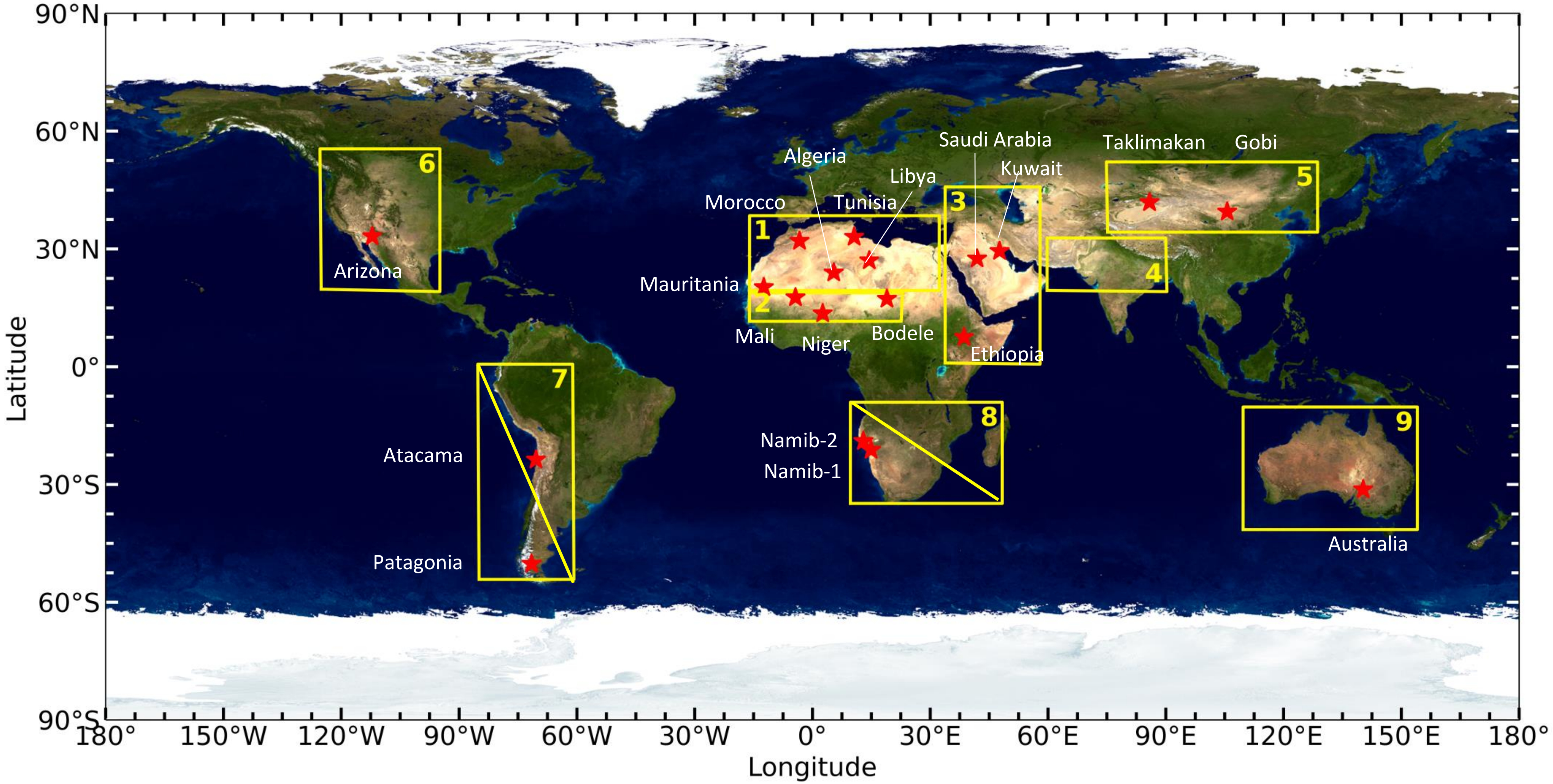

- Yellow rectangular - 9 different global <u>main dust source regions</u> (Ginoux et al., 2012; Di Biagio et al., 2017)
  ((1) northern Africa, (2) the Sahel, (3) eastern Africa and Middle East, (4) central Asia, (5) eastern Asia,
  (6) North America, (7) South America, (8) southern Africa, and (9) Australia)) <u>– (7), (8) MAIAC EPIC do not provide dust</u>

- MAIAC EPIC uses the dust model for known dust source regions (e.g., Sahara, etc.), and the smoke model is applied elsewhere globally.

- Red star – <u>Soil samples</u> collected by Di Biagio et al. (2019). Di Biagio et al. (2019) sampled the 19 sites of source soil and investigated their properties including iron oxides contents, spectral complex refractive indices and spectral SSA.

# Retrieval Results: Dust episodes - Sahara / Sahel

TOA RGB (0-0.55)

$AOD_{443}$ (0-2)

$SSA_{443}$ (0.85-0.98)

SAE(=*b*) (0-4)

$k_0$ (0-0.003)

$C_{M,\ hematite}$ (0-150) [mg/m$^2$]

$C_{M,\ goethite}$ (0-150) [mg/m$^2$]

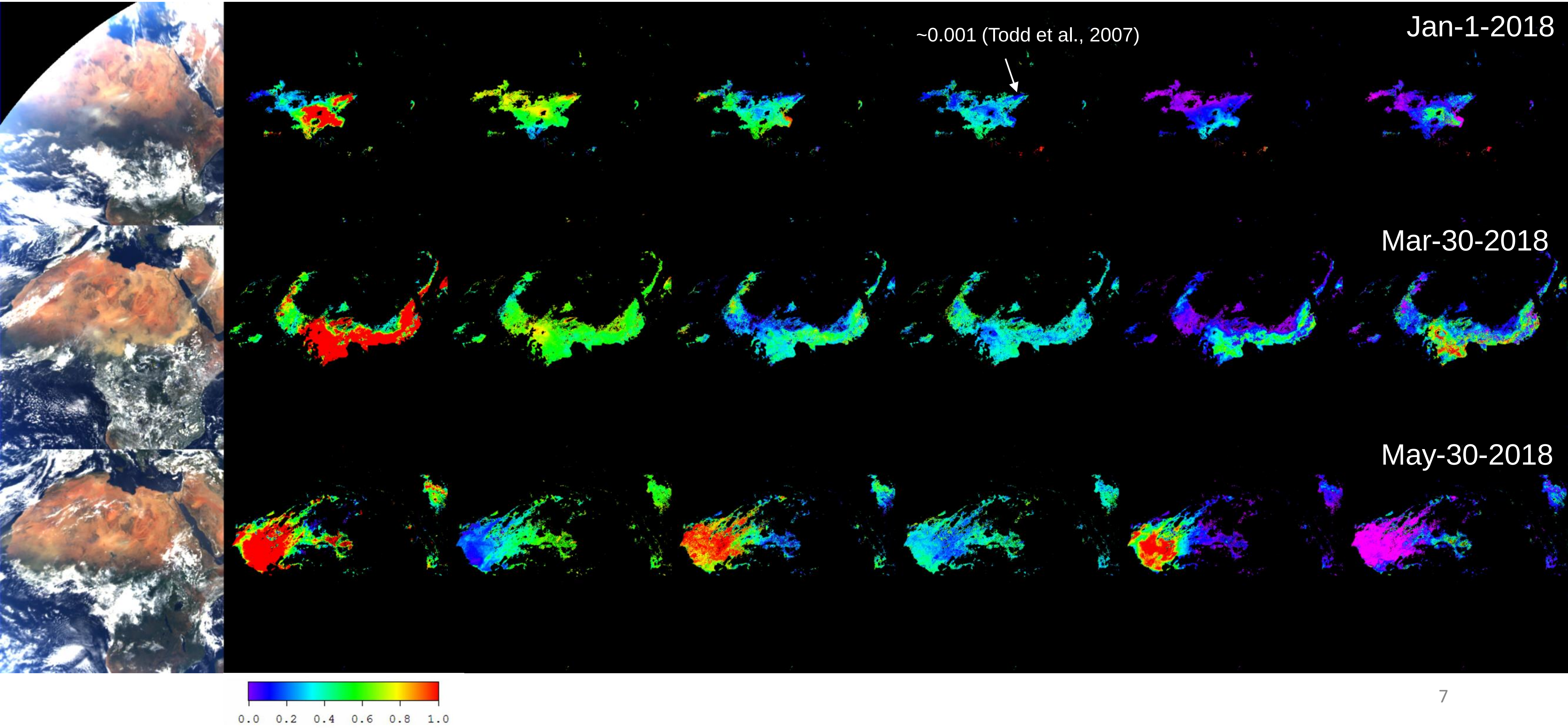

# Comparison with soil measurement data of Di Biagio et al. (2019)

- **Shaded area : EPIC retrieved**
  - Hematite / Goethite
  - 5th, median, 95th
  - With pixels of AOD>1.0 used only
  - ± 1 degree box pixels collected (Monthly)
  - 01/01/2018 – 12/31/2018 (1 year)
  - **Soil content + affected by transport due to different source regions**

- **Dashed line : Di Biagio et al. (2019)**
  - ± 10% uncertainty
  - Simulation chamber study (with X-ray absorption near edge structure (XANES) method), from soil samples and sediments collected from each desert area
  - Refer to the bulk composition of pure dust aerosol in dry condition with a size range of 2-6day transport.
  - **Soil content only**

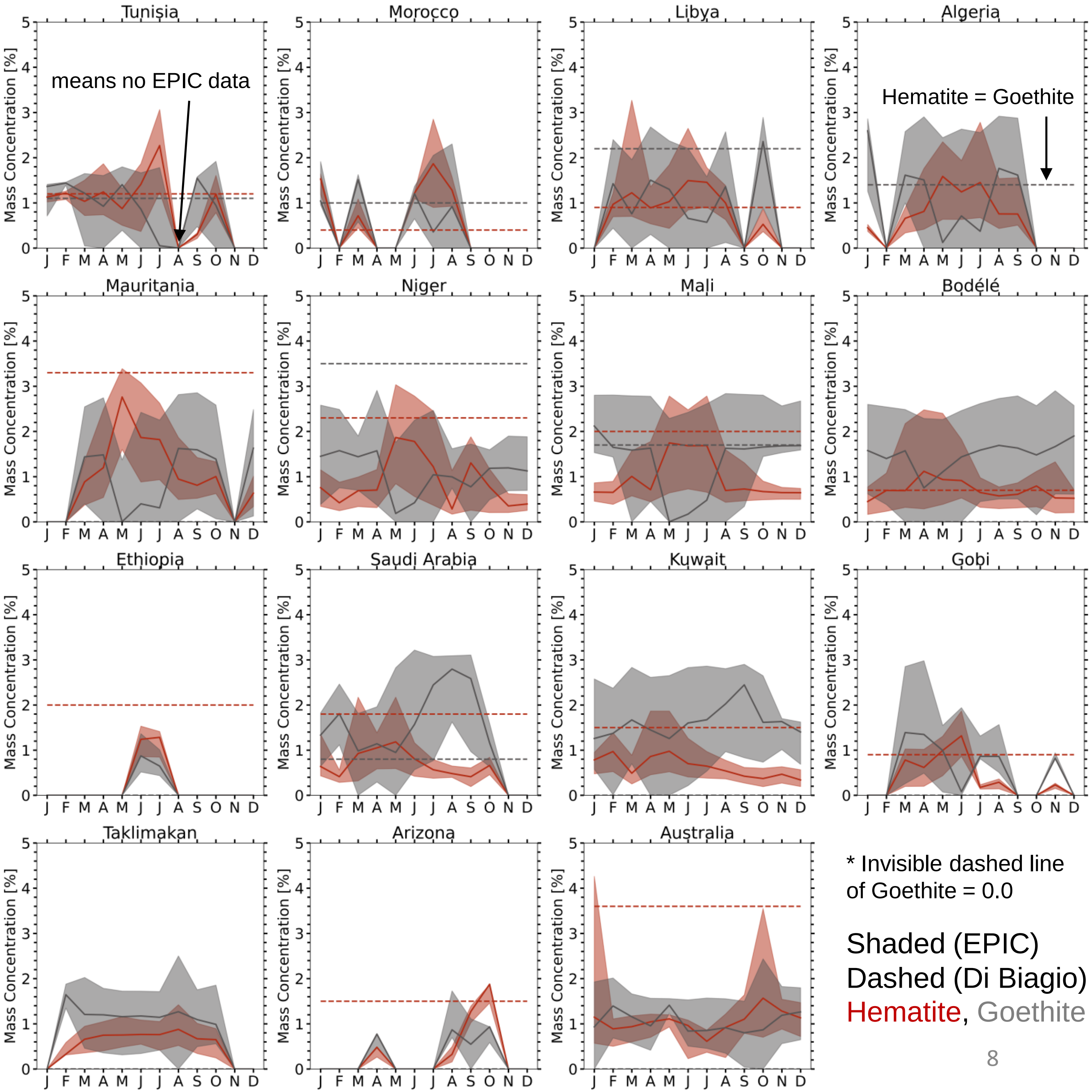

* Invisible dashed line of Goethite = 0.0

Shaded (EPIC)
Dashed (Di Biagio)
Hematite, Goethite

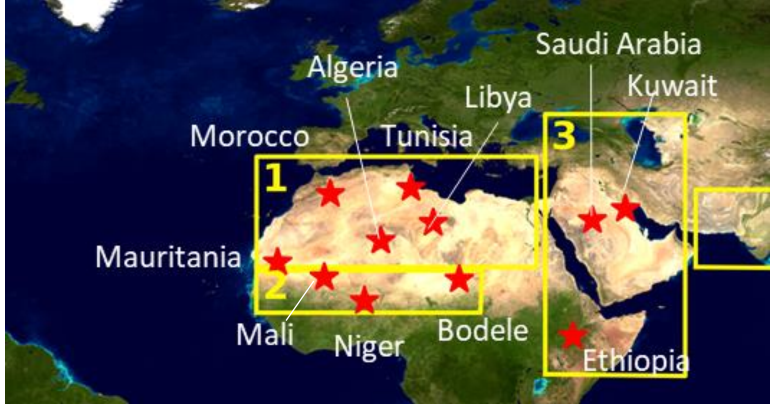

❑ Sahara, Sahel, Middle East → large variability

❑ Sahel line (~20°N) hematite tendency
  - EPIC: Mauritania > Niger > Mali > Bodélé
  - Di Biagio: (3.3%) > (2.3%) > (2.0%) > (0.7%)

❑ Niger (Lafon et al., 2004)
  - Harmattan (11-3): 2.8% iron oxide → agrees
  - Local erosion (5-7): 5.0% (±0.4) iron oxide
    → Possibly due to rain, MAIAC did not catch

❑ Bodélé:
  - EPIC: consistently low hematite (<1.4%)
  - Di Biagio: 0.7% hematite

❑ Saudi Arabia, Kuwait:
  - Shamal season (6-9): northwesterly wind
    → hematite, goethite reversed

❑ Gobi, Taklimakan:
  - Hm/Gt ratio ~ 0.55 observed (Shen et al., 2006)

❑ Arizona, Australia: may contain smoke cases, but case study agreed with dashed line range.

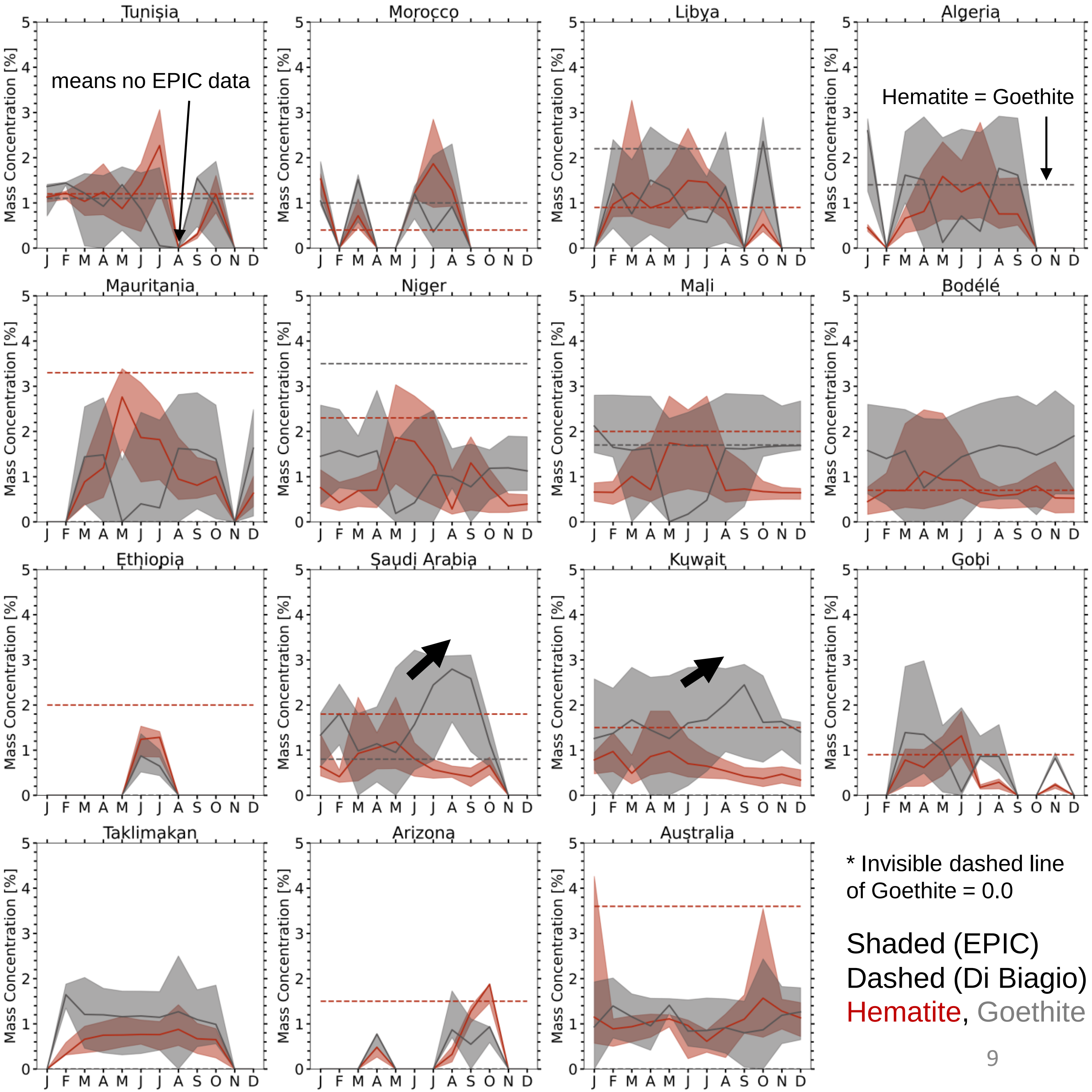

* Invisible dashed line of Goethite = 0.0

Shaded (EPIC)
Dashed (Di Biagio)
Hematite, Goethite

# Hematite refractive indices exhibit a large range in the literature

## 13 different hematite refractive indices

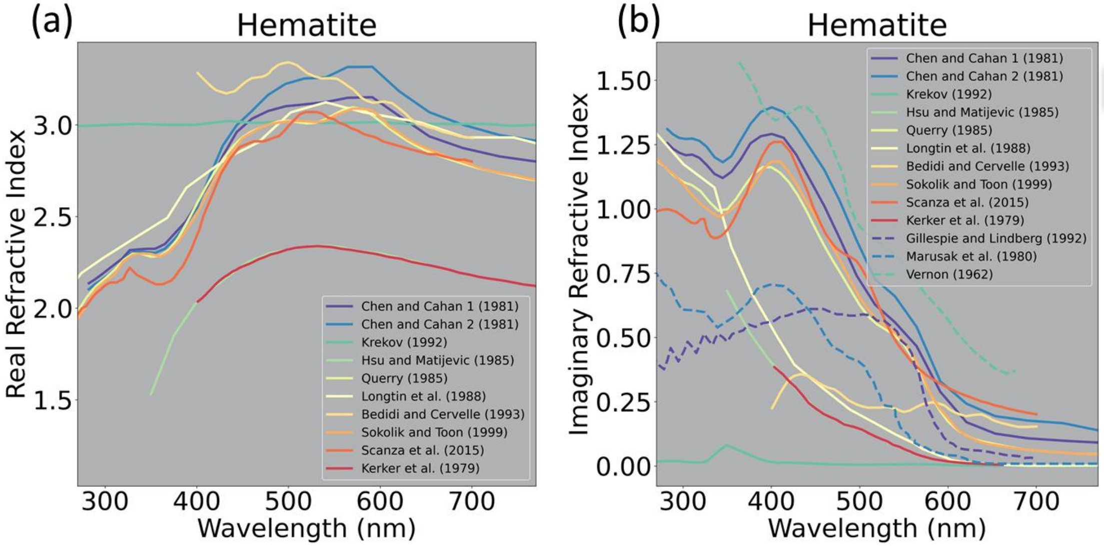

## After exclude: Most suitable hematite refractive index

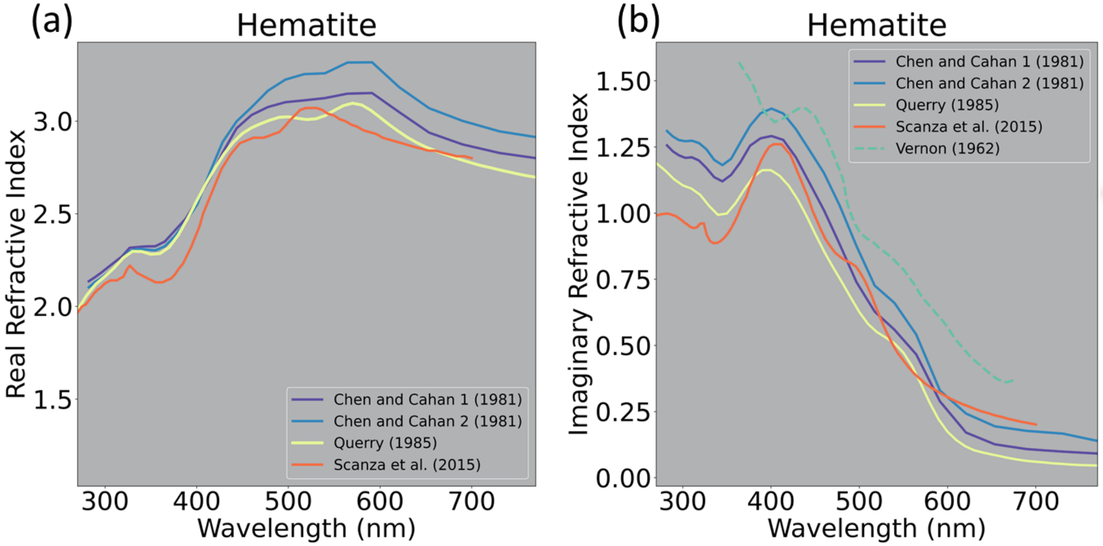

## Same dust event but with
## 13 different models of hematite refractive index

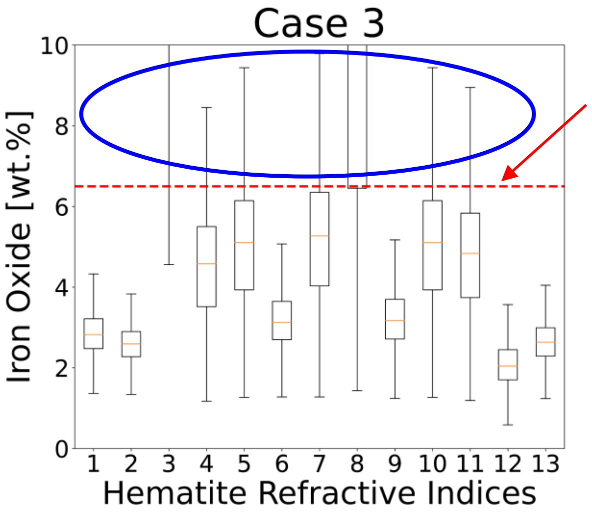

maximum expected iron-oxide content (6.5 wt.%) based on *in situ* measurements

1. Chen and Cahan 1 (1981)
2. Chen and Cahan 2 (1981)
3. ~~Krekov (1992)~~
4. ~~Gillespig and Lindberg (1992)~~
5. ~~Hsu and Matijevic (1985)~~
6. Querry (1985)
7. ~~Longtin (1988)~~
8. ~~Bedidi and Cerville (1993)~~
9. Sokolik and Toon (1999)
10. ~~Kerker (1979)~~
11. ~~Marusak (1980)~~
12. Vernon (1962)
13. Scanza (2015) **– this study**

→ 3,4,5,7,8,10,11 are not viable for our approach

# Smoke episodes – Wildfire Smoke over North America

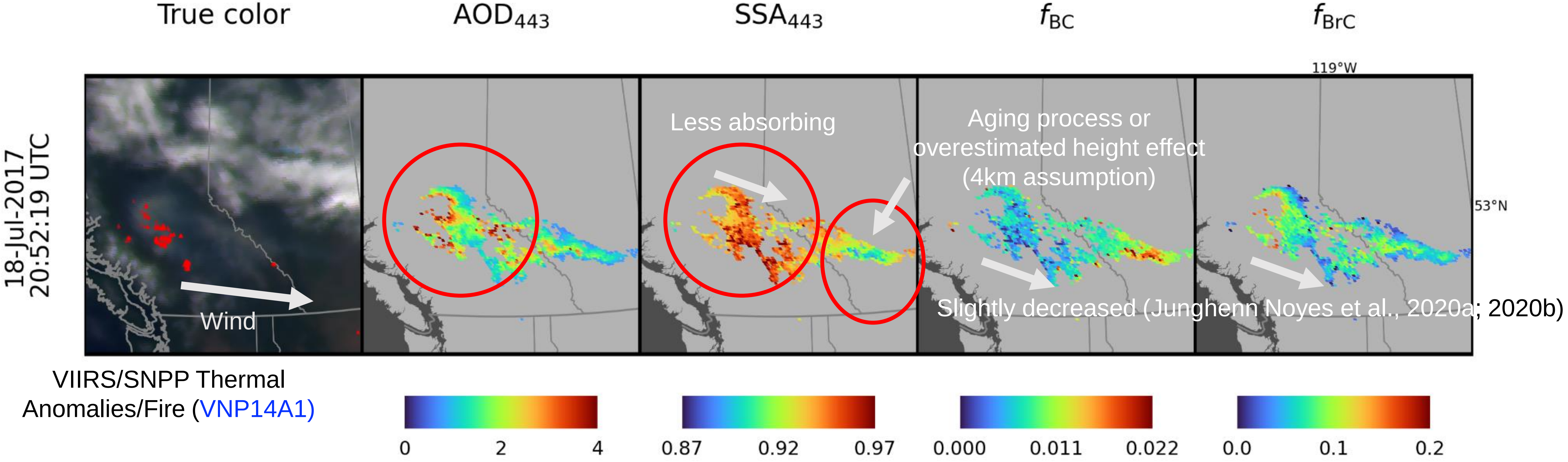

Less absorbing

Aging process or overestimated height effect (4km assumption)

Slightly decreased (Junghenn Noyes et al., 2020a; 2020b)

VIIRS/SNPP Thermal Anomalies/Fire (VNP14A1)

**<Meridional averages of smoke in 2018>**

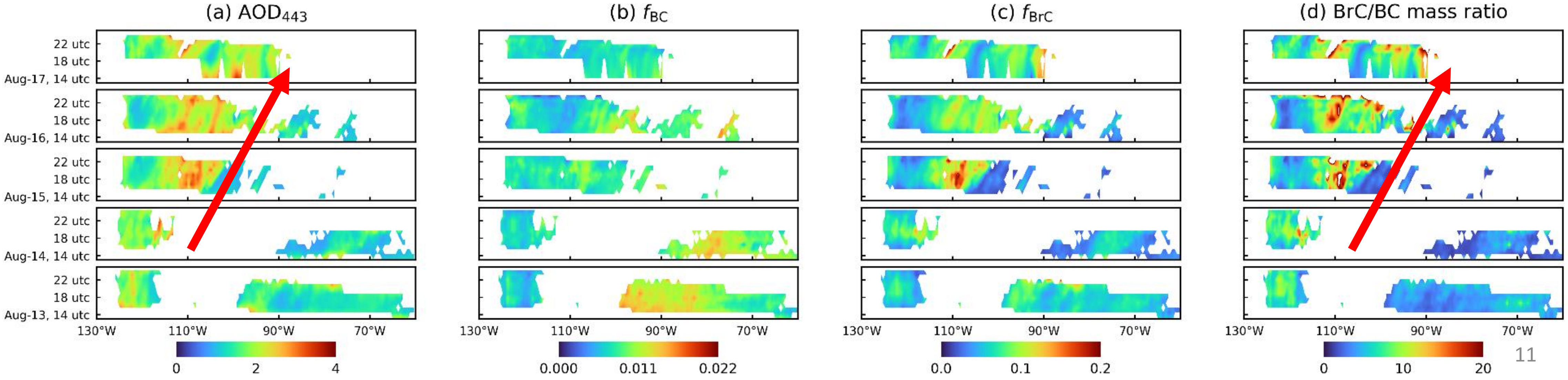

# Climatology of smoke aerosol dominant regions

- ☐ 2015-2020, AOD > 0.6

- ☐ North America
  - High-frequency samples: western US, Canada, BC.
  - High BrC/BC ratio over west US

- ☐ South America
  - Deforestation, climate (El Nino, ENSO related drought)
  - Mean AOD: 1.0-1.8, SSA~0.95
  - relatively low BC (3-5 $mg/m^2$)

  → Agreed with GRASP-component

- ☐ Central Africa
  - Massive source of smoke: wildfire, agricultural, industrial..
  - High number of samples, high BC concentration → Agree with GRASP-component
  - Lower BrC concentration

- ☐ Southeast Asia
  - High AOD, BC, BrC over Laos

  → In line with other studies

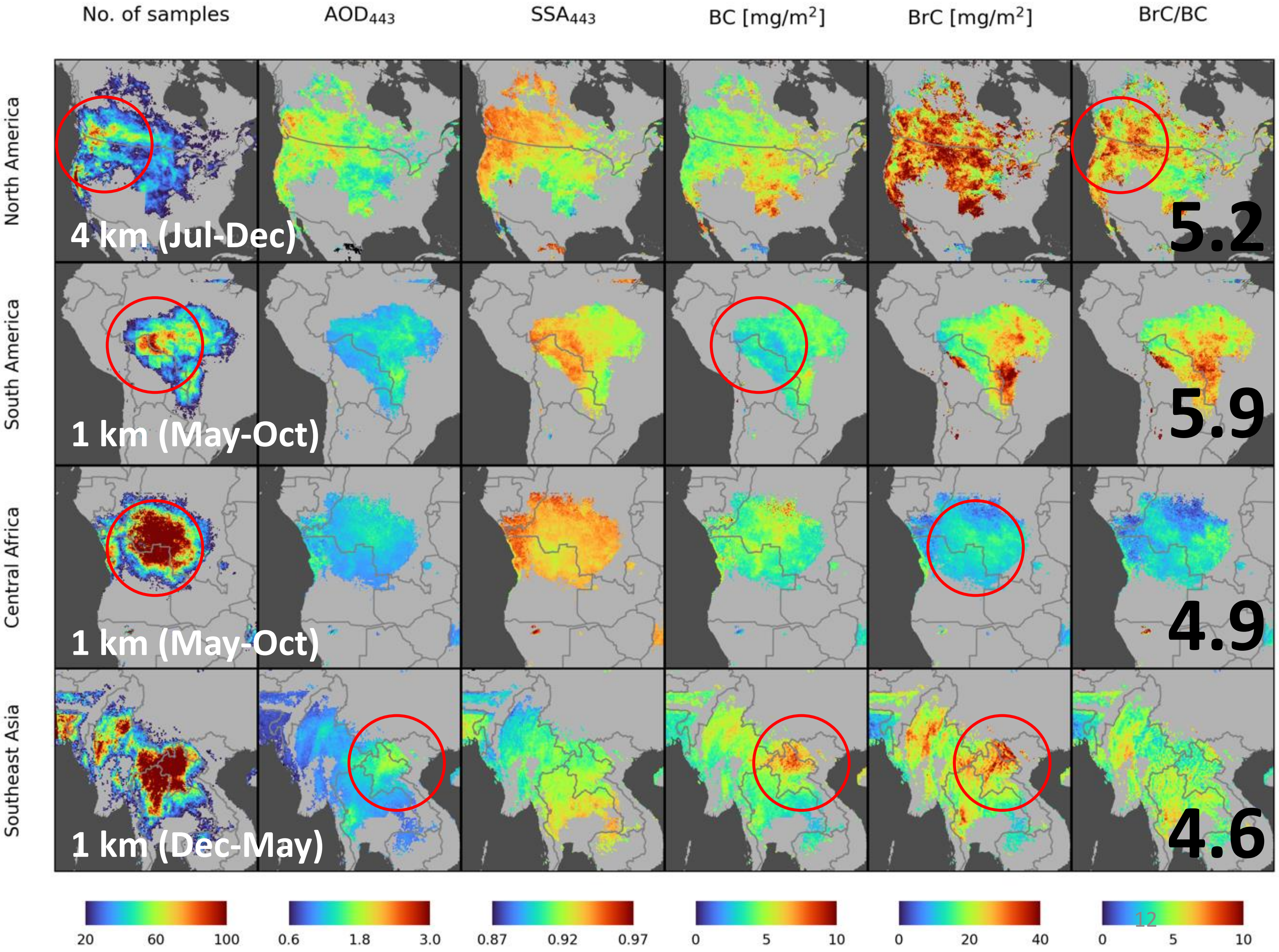

# Conclusion

- Here, contents of hematite (α-Fe2O3) / goethite (α-FeOOH) column for dust (or contents of BC / BrC column for smoke) are inferred from single-viewing satellite EPIC at ultraviolet–visible (UV-Vis) channels globally over major global dust (smoke) source regions using MG EMA internal mixing rule.

- The EPIC MAIAC products are also favorable to monitor a dynamic transport and change of dust/smoke optical properties on a continental scale transport. Retrieved iron oxides enveloped the overall range of Di Biagio et al. (2019) soil measurement data of iron oxides 0.7-5.8% and were in line with the previous published results generally. Combining the VIIRS fire detection and the EPIC MAIAC smoke aerosol products, including BC and BrC, confirmed that freshly emitted smoke aerosols from western North America and Siberia wildfires exhibited high fractions of BC and BrC near sources and the absorption decreased as transported to surroundings.

- The algorithm can be applied for other nadir-viewing instruments having UV-Vis channels, thereby will be beneficial for dust/smoke DRE related climate change (e.g., input for climate models) / air quality (e.g., epidemiology) study.

**[References]**

- **Lyapustin A, Go S, Korkin S, Wang Y, Torres O, Jethva H and Marshak A (2021) Retrievals of Aerosol Optical Depth and Spectral Absorption from DSCOVR EPIC. *Front. Remote Sens*. 2:645794. doi: 10.3389/frsen.2021.645794.**
- **Go, S., Lyapustin, A., Schuster, G. L., Choi, M., Ginoux, P., Chin, M., Kalashnikova, O., Dubovik, O., Kim, J., Silva, A. D., Holben, B., and Reid, J. S.: Inferring iron oxides species content in atmospheric mineral dust from DSCOVR EPIC observations, *Atmos. Chem. Phys. Discuss.* [preprint], https://doi.org/10.5194/acp-2021-599, in review, 2021.**
- **Choi, M., A. Lyapustin, G. Schuster, S. Go, et al. Retrieval of BC and BrC smoke aerosol components from DSCOVR EPIC, *Atmos. Chem. Phys*. (to be submitted, 2021).**